JOURNAL OF MATERIALS SCIENCE LETTERS **21**, 2002, 251 – 255

Organic-inorganic sol-gel coating for corrosion protection of stainless steel

T. P. CHOU
Department of Materials Science and Engineering, University of Washington, Seattle, WA, USA

C. CHANDRASEKARAN
Boston Scientific Northwest Technology Center, Redmond, WA, USA

S. LIMMER, C. NGUYEN, G. Z. CAO
Department of Materials Science and Engineering, University of Washington, Seattle, WA, USA
E-mail: gzcao@u.washington.edu

One of the most effective corrosion control techniques is the electrical isolation of the anode from the cathode [1, 2]. The chromium oxide (Cr_2O_3) passivation layer formed on the surface of stainless steel in oxidizing environments is one example. This is the main reason for the durability and corrosion resistance behavior of this particular metal [2, 3]. A more generic approach to enhance corrosion resistance is to apply protective films or coatings. Through the modification of chemical composition of the coatings, such protective coatings can also permit the introduction of other desired chemical and physical properties, such as mechanical strength and hydrophobicity. Various organic coatings have been studied for corrosion protection [4–6]. Specifically, various oxide coatings by sol-gel processing have been studied extensively for corrosion protection of stainless steel [9–13]. In spite of all the advantages of sol-gel processing, sol-gel oxide coatings suffer from several drawbacks. In general, sol-gel coatings are highly porous with low mechanical integrity; annealing or sintering at high temperatures ($>800\,^{\circ}C$) is required to achieve a dense microstructure [14–17]. Consequently, sintering at high temperatures might introduce cracks and/or delamination of sol-gel coatings due to a large mismatch of thermal expansion coefficients and possible chemical reactions at the interface. Sintering at high temperatures also limits application of sol-gel coatings on temperature sensitive substrates and devices.

One viable approach to dense, sol-gel-derived coatings without post-deposition annealing at elevated temperatures is to synthesize organic-inorganic hybrid coatings. When appropriate chemical composition and processing conditions are applied, relatively dense organic-inorganic hybrid coatings can be developed for applications, including wear resistance [18, 19] and corrosion protection [20–22]. Messaddeq *et al*. [21] studied corrosion resistance of organic-inorganic hybrid coatings on stainless steel. The coatings were made by dispersing various amounts of polymethylmethacrylate (PMMA) into zirconia (ZrO_2) sol and fired at $200\,^{\circ}C$ for 30 min. PMMA-ZrO_2 coatings demonstrated promising corrosion resistance and increased the lifetime of the stainless steel by a factor 30 [21]. However, phase segregation, incomplete coverage, and delamination were observed when the coatings consisted of a high content of organic components. In this paper, we studied the corrosion resistance of sol-gel-derived, organic-inorganic hybrid single-layer coatings on two types of stainless steel. Sol-gel-derived coatings were made from tetraethylorthosilicate (TEOS) and 3-methacryloxypropyltrimethoxysilane (MPS) using a two-step acid catalysis process, and were annealed at $300\,^{\circ}C$ for 30 min. It was demonstrated that sol-gel derived hybrid coatings could significantly enhance the corrosion protection of both 304 and 316 stainless steel substrates. Furthermore, the corrosion resistance behavior of the hybrid coatings on both types of stainless steel was compared and possible mechanisms were discussed.

The silica-based organic-inorganic hybrid sol was prepared with an acid-catalyzed, two-step hydrolysis-condensation process. The hybrid sol was prepared by admixing a silica precursor, tetraethylorthosilicate (TEOS, $Si(OC_2H_5)_4$), and an organic component, 3-methacryloxypropyltrimethoxysilane (MPS, $H_2CC(CH_3)CO_2(CH_2)_3Si(OCH_3)_3$), to control the flexibility and density of the sol-gel network. Silica (SiO_2) sol containing 10 mol% MPS with a TEOS : MPS ratio of 90 : 10 was used for analysis. An initial stock solution was made by adding amounts of TEOS and MPS in a mixture of ethanol (C_2H_5OH), deionized water (DI H_2O), and 1N hydrochloric acid (HCl), resulting in a TEOS : MPS : C_2H_5 : DI-H_2O : HCl nominal molar ratio of $0.90 : 0.10 : 3.8 : 5 : 4.8 \times 10^{-3}$. The mixture was vigorously stirred at a rate of 500 RPM for 90 min at a temperature of $60\,^{\circ}C$, and further processing of the sol required an additional 3.6 mL 1N HCl and 1.2 mL DI H_2O to 30 mL of the stock solution. The sol was stirred again at a rate of 500 RPM for 60 min at a temperature of $60\,^{\circ}C$. Ethanol was added to dilute the sol in order to obtain a volume ratio of 2 : 1 ethanol to solution.

The substrates (10 mm $\times$ 40 mm in dimension) used for the analysis of the sol-gel coatings were 304 and 316 stainless steel that had been electropolished. The exposure of the substrates to nitric acid (HNO_3) decreased the iron content and increased the chromium content

at the surface. In order to ensure a tight bond and good adhesion between the substrate surface and the sol-gel coating, the substrates were exposed to surface hydroxylation at an elevated temperature. Each substrate was initially rinsed with DI H_2O, cleaned with ethanol, and air-dried. The substrates were then immersed for approximately 30 min into a 90 °C solution mixture of 30% hydrogen peroxide (H_2O_2) and concentrated sulfuric acid (H_2SO_4) with a 30 : 70 volume ratio. A DI H_2O rinse was used to wash excess solution remaining and the substrates were then stored in DI H_2O solution to preserve the hydroxyl groups on the surface. Using a dip-coater (Chemat Technology Inc, model 201), each substrate was dipped into the sol at a constant speed of 140 mm/min, immersed into the sol for 1 min, and then withdrawn at approximately the same speed. The coating was air-dried for approximately 1 min and placed in a furnace to initiate post-deposition heat treatment. The single-layer coated substrates were annealed at 300 °C for approximately 30 min at a heating and cooling rate of 5 °C/min. This low temperature annealing process allowed for the preservation of the organic component and the reduction of possible crack formation in the sol-gel coatings due to the difference in thermal expansion coefficients of silica and stainless steel.

All measurements were performed under extreme environmental conditions consisting of an aqueous, air-exposed, saturated sodium chloride (32% NaCl) solution. Each sample was sealed with resistant adhesive tape in order to prevent premature corrosion along the edges of the substrate. A 7.0 mm × 10 mm area within the center of each sample was exposed to the solution during testing. Corrosion analysis of bare and coated substrates was done using a potentiostat (EG&G Instruments Inc, model 273) connected to a corrosion analysis software program (EG&G Princeton Applied Research, model 352/252, version 2.23). Polarization measurements were carried out potentiostatically at room temperature using a saturated calomel reference electrode (SCE) and a platinum counter electrode. The potentiodynamic measurements were taken within the range of −1000 mV to 1200 mV versus SCE at a rate of 2 mV/s. Prior to the measurements, each sample was immersed in 32% NaCl solution for at least 15 min. Optical microscopy and scanning electron microscopy (SEM) were also performed on the bare and coated substrates to characterize the surface morphology. Ellipsometer with a He-Ne laser ($\lambda = 632.8$ nm) was used to determine the relative density and thickness of the sol-gel-derived coatings on silicon wafer.

Optical microscopy and SEM and ellipsometry analyses revealed that uniform, homogeneous, and crack-free hybrid sol-gel coatings on stainless steel substrates were readily obtained prior to and after post-deposition annealing at 300 °C for 30 min. The corrosion protection properties of sol-gel derived coatings are strongly dependent on the processing conditions. In this case, a two-step acid catalyst process was applied in the sol preparation. With this approach, linear silica polymer chains were formed. When dip-coated on a substrate, a sol-gel network based on such linear silica chains would undergo an extensive collapse leading to the formation of dense film upon removal of solvent during drying [23].

Fig. 1a compares the polarization curves of both bare and 10% MPS sol-gel coated 304 stainless steel substrates. A passivation region with a rather low passivation current density of $\sim 3.5 \times 10^{-8}$ A/cm^2 was present in the polarization behavior of the coated substrate, which implied that the sol-gel coating indeed provided a physical barrier for blocking the electrochemical process. Such a barrier would fail only at a high electric potential of ∼770 mV. The bare stainless steel substrate exhibited a significantly different potentiodynamic polarization curve and no obvious passivation region was found. As the electric field increased above its open circuit potential, the current density initially increased rapidly, indicating an active electrochemical reaction. The increase in current density slowed down at a current density of $\sim 10^{-7}$ A/cm^2, indicating the possible formation of a passivation layer. Further increase in electric potential resulted in a rapid increase in the current density.

Fig. 1b compares the polarization curves of both bare and 10% MPS coated 316 stainless steel. A passivation region was present in the polarization behavior of the coated substrate, as evidenced by the constant current density value of $\sim 4.46 \times 10^{-7}$ A/cm^2 with increasing electrical potential. With this low passivation current density, the sol-gel coating resembled a physical barrier for inhibiting the corrosion process. This type of barrier would break down only at a greater electric potential of ∼1100 mV. On the other hand, the bare stainless steel substrate exhibited a significantly different potentiodynamic polarization curve. Possible passivation and repassivation behavior was found. An initial increase in the electric potential increased the current density rapidly, indicating an active electrochemical reaction. At $\sim 10^{-6}$ A/cm^2, a continued increase in the electric potential decreased the current density, indicating the possible formation of a passivation layer. Further increase in electric potential resulted in a quick increase in current density resulting from the electrochemical reaction. Repassivation behavior was also present during slow increases in the current density at higher electric potentials.

In both cases, the polarization curves of the sol-gel coated substrates were appreciably different from that of the bare stainless steel substrates indicating that the hybrid coating had an effect on the corrosion behavior. The open circuit potential, E_{oc}, of the sol-gel coated substrates was significantly lower than that of the bare stainless steel substrates. This reduction in open circuit potential might be due to the effective suppression of the cathodic reaction (SiO_2 has a low isoelectric point, leading to a negative surface charge at pH > 2 [14, 24]). In addition, a distinct passivation region was present for the coated substrates, whereas no definitive passivation region was found for the bare stainless steel substrates.

After the electrochemical polarization tests, the samples were closely analyzed by SEM. It was found that the 304 stainless steel substrate with hybrid coating showed extensive pitting from electrochemical reactions along the surface. The delamination and

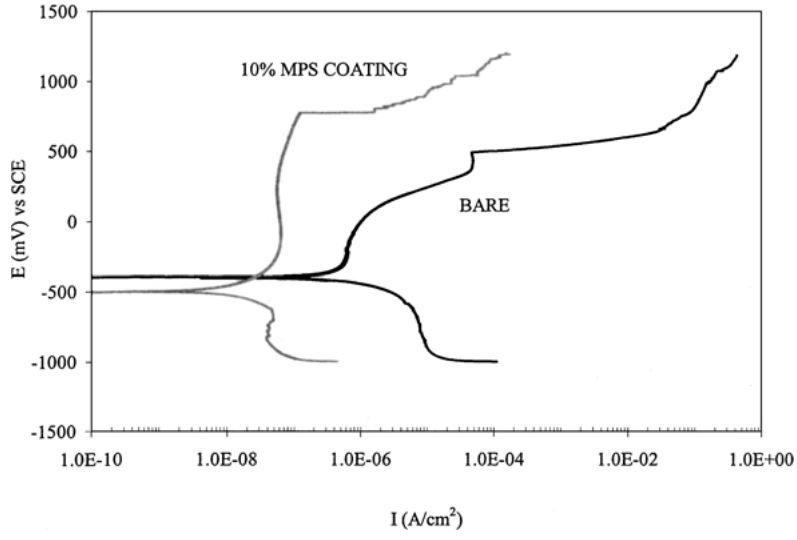

(a)

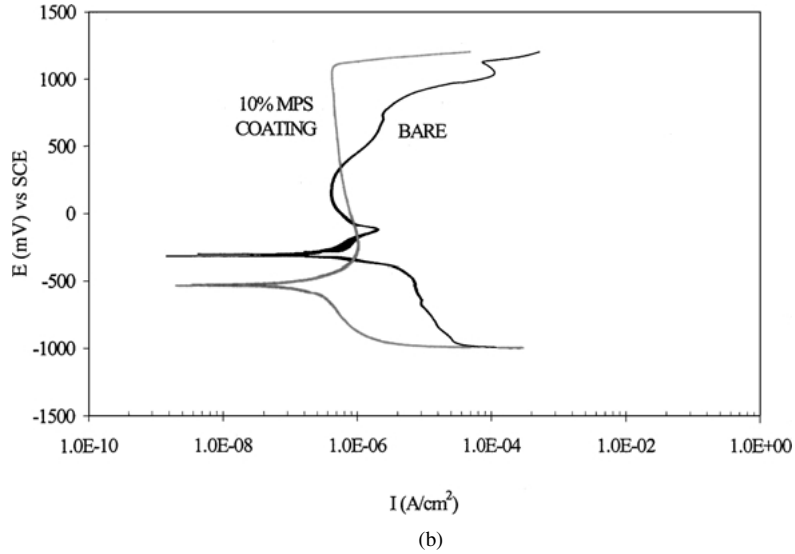

(b)

Figure 1 (a) Polarization curves of bare and organic-inorganic hybrid film coated 304 stainless steel substrates; and (b) polarization curves of bare and organic-inorganic hybrid film coated 316 stainless steel substrates.

breakdown of the coating could be clearly seen along the edge and interior of the corrosion pits, indicating preferential localized attack. The 316 stainless steel substrate with hybrid coating, on the other hand, showed no signs of pitting along the surface. The SEM image showed a smooth stainless steel surface with no appreciable delamination or cracking of the coating on the 316 stainless steel substrate. Fig. 2 shows the SEM images of the 304 and 316 stainless steel substrates coated with the same hybrid sol-gel films after the electrochemical polarization tests. Fig. 2a shows that electrochemical reactions along the surface of 304 stainless steel substrate caused extensive localized delamination and separation of the coating from the substrate. The presence of the coating along the edges and along the interior of the pit indicated that there was definitely debonding and lifting of the coating from the substrate, which resulted in the breakdown. In contrast, Fig. 2b shows that there was neither pitting nor delamination of the hybrid coating on the 316 stainless steel substrate after the electrochemical polarization test. This indicates that electrochemical reaction along the interface between the hybrid coating and the 316 substrate was different from that of 304 substrate.

It is not clear why the same sol-gel-derived, organic-inorganic hybrid coatings exhibited appreciably different corrosion behavior. One plausible explanation would be due to the different substrates. Although the hybrid coatings are relatively dense, there are microscopic pores as evidenced by carbon dioxide sorption isotherms [25, 26]. Some corrosive ions such as chlorine anions would be able to diffuse through these microscopic pores and react with metal elements at the interface between the hybrid coating and substrate. This corrosion process at the interface would be strongly dependent on the nature of substrates and may result in corrosion patterns.

Fig. 3 illustrates possible mechanisms of corrosion for the two types of stainless steel substrates based on the SEM images. In this figure, for the sake of simplicity, only the Fe element is considered in the electrochemical reactions. It is well known, however, that other metals, particularly Cr and Mo, would certainly participate to the reactions and contribute significantly

(a)

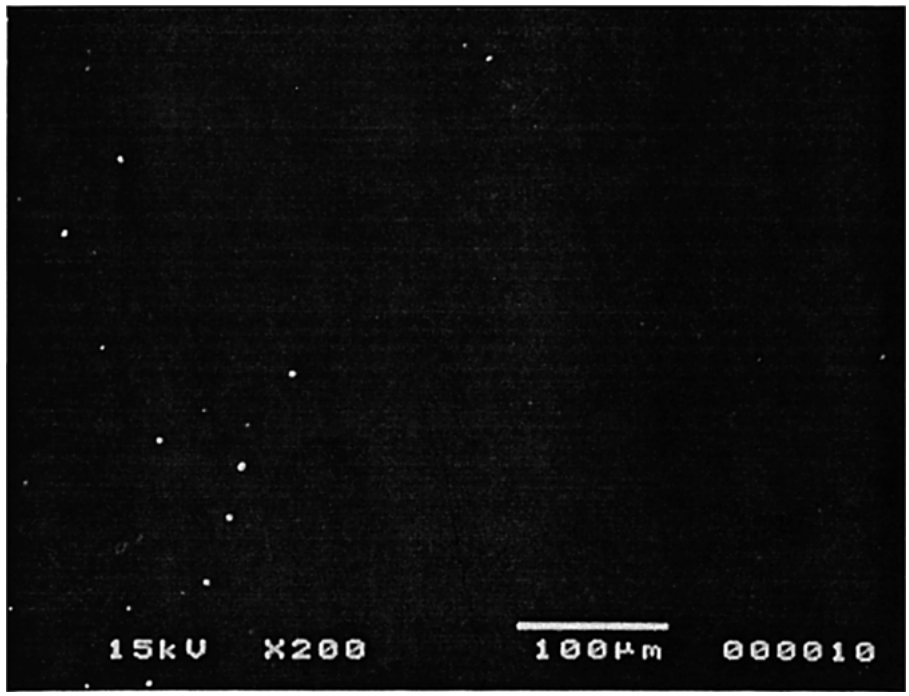

(b)

Figure 2 SEM images of the top morphology of the organic-inorganic hybrid films coated (a) 304 stainless steel substrate and (b) 316 stainless steel substrate after polarization analyses.

to the corrosion mechanisms. Fig. 3a depicts the possible corrosion mechanism of sol-gel coatings on the 304 stainless steel substrate. The localized electrochemical reaction at the interface resulted in debonding, delamination and lifting of the sol-gel coating from the substrate due to a volume expansion as a result of metal oxidation. Delamination between the sol-gel coating and the substrate could be attributed at least partly to hydrolysis reactions at the interface, which was also found at the interface between sol-gel coatings and polyester substrates [18]. Fig. 3b suggests a possibly different corrosion mechanism at the interface between the sol-gel coating and 316 stainless steel substrate. Comparison of corrosion curves of bare 304 and 316 stainless steel substrates (Fig. 1) reveals that a passivation film on the surface of 316 substrate was possibly formed during the electrochemical test; however, such a passivation film was less likely formed on the surface of 304 substrates. Furthermore, compared to 304 stainless steel, 316 stainless steel contains additional 2–3% molybdenum and, thus, possesses better corrosion resistance [27]. Therefore, it is possible that the electrochemical reaction between of corrosive ions and the metal elements at the interface between the sol-gel

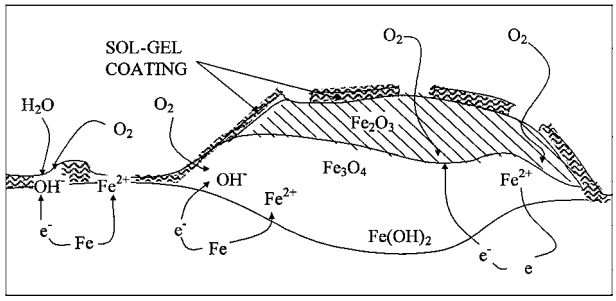

(a)

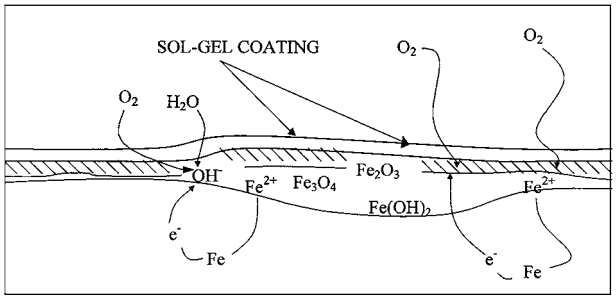

(b)

Figure 3 Schematic illustration of simplified possible corrosion mechanisms: (a) hybrid coating on 304 stainless steel and (b) hybrid coating on 316 stainless steel. For the sake of simplicity, only Fe element is used to illustrate the electrochemical reactions.

coating and 316 substrate resulted in the formation of a uniform oxide layer.

In summary, silica-based hybrid coatings, prepared by a two-step acid catalyst sol-gel process, were found uniform, defect-free, and relatively dense. Hybrid coatings on stainless steel substrates enhanced corrosion protection by forming a physical barrier, which effectively separated the anode from the cathode electrically. However, corrosive ions could still diffuse through micropores in the sol-gel coatings and react with the metal elements at the interface between the sol-gel coating and substrate. Corrosion mechanisms were found to be strongly dependent on the nature of substrates.

Acknowledgments

The authors would like to acknowledge the partial financial support from Boston Scientific Northwest Technology Center and Center for Nanotechnology at UW through NSFIGERT fellowship (S. J. Limmer) as well as the technical support from Dave Rice and Sam Salamone.

References

1. D. A. JONES, "Principles and Prevention of Corrosion," 2nd ed. (Prentice-Hall, New Jersey, 1996).
2. L. L. SHREIR, R. A. JARMAN and G. T. BURSTEIN (Eds.), "Corrosion," 3rd ed. (Butterworth-Heinemann, Oxford, 1994).
3. R. BUCHHEIT, *J. Electrochem. Soc.* **142** (1994) 3994.
4. G. GRUNDMEIER, W. SCHMIDT and M. STRATMANN, *Electrochimica Acta* **45** (2000) 2515.
5. R. HANEDA and K. ARAMAKI, *J. Electrochem. Soc.* **145** (1998) 2786.
6. W. LU, R. L. ELSENBAUMER, T. CHEN and V. G. KULKARNI, *Mat. Res. Soc. Symp. Proc.* **488** (1998) 653.
7. R. HANEDA and K. ARAMAKI, *J. Electrochem. Soc.* **145** (1998) 1856.
8. M. ITOH, H. NISHIHARA and K. ARAMAKI, *ibid.* **142** (1995) 3696.
9. M. GUGLIELMI, *J. Sol-Gel Sci. Tech.* **1** (1994) 177.
10. D. C. L. VASCONCELOS, J. N. CARVALHO, M. MANTEL and W. L. VASCONCELOS, *J. Non-Cryst. Solids* **273** (2000) 135.
11. M. SIMOES, O. B. G. ASSIS and L. A. AVACA, *ibid.* **273** (2000) 159.
12. M. ATIK, S. H. MESSADDEQ, F. P. LUNA and M. A. AEGERTER, *J. Mater. Sci. Lett.* **15** (1996) 2051.
13. P. NETO, M. ATIK, L. A. AVACA and M. A. AEGERTER, *J. Sol-Gel Sci. Tech.* **2** (1994) 529.
14. C. J. BRINKER and G. W. SCHERER, "Sol-Gel Science: The Physics and Chemistry of Sol-Gel Processing" (Academic Press, San Diego, CA, 1990).
15. A. C. PIERRE, "Introduction to Sol-Gel Processing" (Kluwer, Boston, MA, 1998).
16. L. F. FRANCIS, *Mater. Manufacturing Process.* **12** (1997) 963.
17. X. H. HAN, G. Z. CAO, T. PRATUM, D. T. SCHWARTZ and B. LUTZ, *J. Mater. Sci.* **36** (2001) 985.
18. C. M. CHAN, G. Z. CAO, H. FONG, M. SARIKAYA, T. ROBINSON and L. NELSON, *J. Mater. Res.* **15** (2000) 148.
19. J. WEN and G. L. WILKES, *J. Inorganic and Organometallic Polymers* **5** (1995) 343.
20. J. S. PARK and J. D. MACKENZIE, *J. Amer. Ceram. Soc.* **78** (1995) 2669.
21. S. H. MESSADDEQ, S. H. PULCINELLI, C. V. SANTILLI, A. C. GUASTALDI and Y. MESSADDEQ, *J. Non-Cryst. Solids* **247** (1999) 164.
22. M. ATIK, F. P. LUNA, S. H. MESSADDEQ and M. A. AEGERTER, *J. Sol-Gel Sci. Tech.* **8** (1997) 517.
23. C. J. BRINKER, A. J. HURD, P. R. SCHUNK, G. C. FRYE and C. S. ASHLEY, *J. Non-Cryst. Solids* **147/148** (1992) 424.
24. R. K. ILER, "The Chemistry of Silica: Solubility, Polymerization, Colloid and Surface Properties, and Biochemistry" (John Wiley & Sons, New York, 1979).
25. G. Z. CAO, Y. F. LU, L. DELATTRE, C. J. BRINKER and G. P. LÓPEZ, *Adv. Mater.* **8** (1996) 588.
26. Y. F. LU, G. Z. CAO, R. P. KALE, S. PRABAKAR, G. P. LÓPEZ and C. J. BRINKER, *Chem. Mater.* **11** (1999) 1223.
27. G. S. BRADY, H. R. CLAUSER and J. A. VACCARI (Eds.), "Materials Handbook," 14th ed. (McGraw-Hill, New York, 1997).

Received 18 August
and accepted 18 October 2001